Thickness-dependent electronic structure in ultrathin LaNiO_{3} films under tensile strain

Hyang Keun Yoo, Seung Ill Hyun, Young Jun Chang, Luca Moreschini, Chang Hee Sohn,
Hyeong-Do Kim, Aaron Bostwick, Eli Rotenberg, Ji Hoon Shim, and Tae Won Noh

Thickness-dependent electronic structure in ultrathin LaNiO₃ films under tensile strain

Hyang Keun Yoo[1,2], Seung Ill Hyun[3], Young Jun Chang[4,5], Luca Moreschini[5], Chang Hee Sohn[1,2], Hyeong-Do Kim[1,2*], Aaron Bostwick[5], Eli Rotenberg[5], Ji Hoon Shim[3,6] and Tae Won Noh[1,2]

[1]Center for Correlated Electron Systems, Institute for Basic Science (IBS), Seoul 151-747, Republic of Korea.

[2]Department of Physics and Astronomy, Seoul National University, Seoul 151-747, Republic of Korea.

[3]Department of Chemistry, Pohang University of Science and Technology, Pohang 790-784, Republic of Korea.

[4]Department of Physics, University of Seoul, Seoul 130-743, Republic of Korea.

[5]Advanced Light Source, Lawrence Berkeley National Laboratory, Berkeley, California 94720, USA.

[6]Division of Advanced Nuclear Engineering, Pohang University of Science and Technology, Pohang 790-784, Republic of Korea.

*e-mail: hdkim6612@snu.ac.kr

We investigated electronic-structure changes of tensile-strained ultrathin LNO films from 10 to 1 unit cells (UC) using angle-resolved photoemission spectroscopy (ARPES). We found that there is a critical thickness t_c between 4 and 3 UC below which Ni e_g electrons are confined in two-dimensional space. Furthermore, the Fermi surfaces (FSs) of LNO films below t_c consist of two orthogonal pairs of one-dimensional (1D) straight parallel lines. Such a feature is not accidental as observed in constant-energy surfaces at all binding energies, which is not explained by first-principle calculations or the dynamical mean-field theory. The ARPES spectra also show anomalous spectral behaviors, such as no quasiparticle peak at Fermi momentum but fast band dispersion comparable to bare-band one, which is typical in a 1D system. As its possible origin, we propose 1D FS nesting, which also accounts for FS superstructures observed in ARPES.

I. INTRODUCTION

Dimensionality and strain control is at the heart of ultrathin-film engineering [1-8]. As the film thickness t approaches one unit cell (UC), quantum confinement restricts electronic motion within a two-dimensional (2D) plane [5-7]. In a strongly correlated transition-metal oxide (TMO), such 2D confinement is crucial in determining its electronic properties due to the balance between electronic kinetic motion and correlation [9]. Thus, the dimensionality can be used as a key parameter to control various physical properties of TMOs. Additionally, because quantum correlation becomes strong in lower dimension, it can drive a TMO film to reach a novel quantum phase [10,11]. In recent decades, a lot of studies have been devoted along this direction to search for new interesting phenomena [3,5-8]. However, fundamental understandings on the phenomena appearing at ultrathin TMO films remain challenging [5-7]. This is due, in part, to the difficulty in preparing high-quality ultrathin films and measuring their electronic structures *in situ* by state-of-the-art spectroscopy techniques, such as angle-resolved photoemission spectroscopy (ARPES).

Among numerous TMOs, LaNiO$_3$ (LNO) has recently attracted much interest, partly due to its potential electronic analogue to high-T_c cuprate superconductors under the conditions of tensile strain and reduced dimensionality [12-14]. Although superconductivity in nickelates has not yet been realized and theoretical controversy has been provoked [15,16], other interesting results have been reported upon reducing its dimensionality. Among them, observation of a metal-insulator transition (MIT) [17-19] and a spin/charge ordering [20-22] below a critical thickness t_c have drawn much attention. These phenomena were proposed to originate from novel electronic phases attained by changing the dimensionality. Direct observations of their electronic structures followed, but the results are controversial. Using soft X-ray photoemission spectroscopy, Sakai *et al*. [23] observed "gradual" localization of Ni $3d$ electrons in "compressively strained" ultrathin LNO films on a LaAlO$_3$ substrate. In

contrast, King *et al.* [24] by ARPES using He I & II radiation, reported "abrupt" destruction of Fermi-liquid-like quasiparticles on a similar LNO film, which was attributed to a fluctuating spin order enhanced by quantum confinement.

Here, we investigate the electronic structures of "tensile-strained" ultrathin LNO films using in situ ARPES utilizing synchrotron radiation. By reducing the LNO film thickness consecutively from 10 to 1 UC, we found "abrupt" changes of the electronic structures at a critical thickness t_c, consistent with earlier resistivity measurements [20,21]. However, the Fermi-surface (FS) topology is quite different from that of high-T_c cuprate superconductors, and the ARPES spectra unexpectedly show finite spectral weight at the Fermi level (E_F) even in the insulating phase. Furthermore, below t_c between 3 and 4 UC, e_g electrons behave as if they are not only confined in a 2D plane but also moving along a one-dimensional (1D) line. Such a 1D characteristic cannot be easily derived from an e_g-orbital manifold. We suggest that this bizarre behavior could be explained by 1D FS nesting. Thus, ultrathin LNO films provide an intriguing platform to investigate anomalous properties in strongly correlated TMO films.

II. METHODS

High-quality epitaxial LaNiO$_3$/LaAlO$_3$/Nb:SrTiO$_3$ films were fabricated using pulsed laser deposition (PLD). We used a KrF excimer laser ($\lambda = 248$ nm) with a repetition rate of 2 Hz to ablate sintered stoichiometric targets. The laser energy density was 1~1.5 J cm^{-2} at the target position. Before PLD, atomically flat 0.5 wt %-Nb-doped SrTiO$_3$ (STO) substrates were prepared using buffered-HF etching and heating processes. The STO substrates were conducting due to Nb doping, which prevented charging problems during the ARPES measurements. Additionally, to avoid possible intermixing between La and Sr, we deposited a 15-UC-thick LaAlO$_3$ buffer layer. Finally, we deposited 1 UC to 10 UC of LaNiO$_3$ (LNO)

films by monitoring the film thickness with *in situ* reflection high-energy electron diffraction. To prevent quality variation among films, we deposited all of the films between 1 and 10 UC at once by selectively choosing the deposited area using a mechanical shutter, called by "staircase structure". We confirmed that a 30-UC-thick LNO film grown on STO under the same deposition conditions was fully and homogeneously strained (tensile misfit strain of +1.7 %) using synchrotron-based X-ray diffraction at the 9C Beamline of Pohang Light Source. Therefore, all of the ultrathin LNO films used in this study should have been fully strained under tensile misfit strain.

All measurements were performed at an end-station equipped with ARPES and PLD at the Beamline 7.0.1 of the Advanced Light Source. After deposition, the thin films were transferred without breaking a vacuum to an analysis chamber with a base pressure of 5×10^{-11} Torr. The sample temperature was kept at 90 K, except for the cases specified. The total-energy resolution was about 30 meV at $h\nu = 150$ eV. ARPES measurements were carried out in the ΓXM and the ZRA symmetry planes at $h\nu = 157$ and 120 eV, respectively, which were determined by varying the photon energy at normal emission.

III. Results and Discussion

A. Abrupt electronic-structure change by dimensionality control

We investigated how the electronic structure of a tensile-strained LNO film evolves with thicknesses ranging from 10 to 1 UC by ARPES. Because we are dealing with ultrathin films, it may be plausible to use surface Brillouin zone notation. However, our 10 UC LNO film exhibits a three-dimensional (3D) electronic structure with electron and hole pockets located at the Γ and A points, respectively [25]. These are consistent with band-calculation results for bulk LNO [26] and the results from an earlier soft x-ray ARPES study [27] on a much thicker

(about 50 UC) film. Thus, for convenience, we use the notation for a bulk tetragonal structure.

Figure 1 shows the thickness-dependent electronic structures of LNO films measured by ARPES. As the thickness decreased down to 4 UC, we can see some gradual changes, but their spectral features remain essentially the same. Note that ARPES measures only the topmost several layers due to short photoelectron escape depth. Additionally, the thickness of a thin-film thickness may not be so uniform over the measured area. This may explain the "gradual" localization in the experimental ARPES spectra in Ref. 23, in which the photoelectron escape depth was somewhat larger than those of other ARPES measurements [24], including ours.

However, another 1 UC reduction from 4 UC results in dramatic electronic-structure changes as follows. (1) FSs in the ΓXM and the ZRA planes become nearly identical as shown in Figs. 1(d)-(f). (2) The band dispersions along the ΓXM and the ZRA lines are also nearly the same [Figs. 1(j)-(l)]. (3) Strongly renormalized quasiparticle peaks along the ΓXM and the ZRA lines in thick films disappear. Instead, a faint but fast band appears. (4) The size of the electron pocket at the Γ point becomes smaller but does not vanish. Momentum distribution curve (MDC) plots in Supplemental Material (SM) Fig. S2 show more clearly that these abrupt electronic-structure changes take place at t_c between 4 and 3 UC [28].

The observations (1) and (2) imply that the k_z dependence in the electronic structure disappears, indicating that that the 3D electronic structures in the thick ($t > t_c$) films become 2D-like ones at $t < t_c$. The critical thickness value is consistent with our resistance measurements (SM Fig. S4) that show a MIT at t_c. Thus, we conclude that there is an abrupt electronic phase transition at t_c. Our critical-thickness value is 1 UC larger than that reported in previous ARPES study [24]. However, the overall features of the spectral changes are similar. The difference may originate from a reduced strain in our study. Note that our results are consistent with other resistivity measurements using $SrTiO_3$ substrates [20,21].

B. Electronic analogue to high-T_c cuprates?

Even though bulk LNO is a simple paramagnetic metal at all temperatures [29], it has attracted much attention because of its potential to be an electronic analogue to high-T_c cuprate superconductors via strain and dimensionality control [12-14]. Now, our LNO films below t_c will be a good test bed for this theoretical proposal, because it is under 1.7% tensile strain and well-confined in 2D. According to the observation (4) in the previous section, the electron pocket at the Γ point does not vanish even at 1 UC though its volume gradually decreases. Thus, we can conclude that the high-T_c cuprate-like electronic structure in ultrathin LNO films is difficult to achieve at least under these conditions. We can think of hole doping for this end to push away the electron pocket, but it will be a more difficult task because a formally Ni^{4+} or O^{1-} ion is chemically unfavorable.

The original proposal is based on the effective two-band Hubbard model solved by the dynamical mean-field theory (DMFT) [13,14]. The single-band physics as in cuprates [30] could be achieved by large crystal-field splitting and quantum confinement. However, if the O $2p$ degrees of freedom are explicitly taken into account, then the orbital polarization is not so considerable as in the two-band model and the FS topology does not change [15]. Such behavior was examined by thorough comparison of both models, and attributed to the Hund's coupling between two d electrons that plays an important role when about one electron is transferred from the O $2p$ orbitals [16]. Our ARPES results strongly suggest that the charge-transfer energy in LNO is so small or negative that the O $2p$ degrees of freedom cannot be integrated out.

C. Anomalous electronic structure below t_c

As shown in Figs. 1(d)-(f), FSs in LNO films below t_c are comprised of pairs of parallel

straight lines along the k_x- and k_y-axes. These parallel lines in the k_x-k_y plane are the signature of quasi-1D nature in the electronic structure [31,32]. Additionally, the essentially identical band dispersions along the $X\Gamma X$ and the MXM lines for $t < t_c$ [Fig. 2(a)] provide further compelling evidence for the quasi-1D nature. In contrast, Fig. 2(b) shows different band dispersions along the same symmetry lines for the 10 UC film. The band calculations using the generalized gradient approximation (GGA) for the 1 UC LNO, show that the band along the $X\Gamma X$ line has a strong $3z^2$-r^2 character, whereas the band along the MXM line a heavily mixed orbital character of $3z^2$-r^2 and x^2-y^2, as shown in Fig. 2(e). Thus, the dispersion along the MXM line for $t > t_c$ should be much faster than that along the $X\Gamma X$ line, as shown in Fig. 2(b). Despite different orbital characters, the nearly same band dispersions in Fig. 2(a) suggest that there should be some underlying mechanism for such unexpected behavior.

To determine whether or not the band dispersions are truly 1D-like over the entire energy-momentum space, constant-energy-surface (CES) maps for the 2 UC film are depicted in Fig. 2(c) (ΓXM plane) and 2(d) (ZRA plane) down to −0.4 eV in increments of −0.1 eV. If the quasi-1D-like fermiology is accidental, then the CES maps at deeper binding energies should show a dispersive 2D shape in the k_x-k_y plane. Quite surprisingly, the pair of two parallel straight lines is well preserved at all binding energies, with only broadening and a slight reduction in the distance between them. These results strongly suggest that the abrupt change in the electronic structure at t_c is related not only to 2D quantum confinement but also to the quasi-1D behavior.

Figure 2(e) shows CES maps calculated using the GGA for a 1 UC LNO. In contrast to the measurements, the 2D nature of the electronic structure is quite evident. To determine whether or not the quasi-1D behavior can be explained by local correlation effects, we performed dynamical mean-field theory calculations combined with the GGA (GGA+DMFT). As depicted in Fig. 2(f), the fermiology is somewhat similar to the ARPES results except a

8

slight gap between the electron and the hole pockets along the ΓM line. However, the CES map at -0.1 eV deviates significantly from the 1D nature. CES maps from the GGA+DMFT calculations at higher binding energies are similar to those shown in Figs. 2(c) and 2(d). However, these features arise from incoherent excitations, because the minimum of the quasiparticle dispersion is located at about -0.2 eV (SM Fig. S5). Thus, the 1D-like behavior cannot be explained within the DMFT picture.

D. Anomalous single-hole dynamics

Along with the anomalous behavior in the fermiology and the band dispersions below t_c, we also observed peculiar spectral features in ARPES. Figure 3 compares ARPES spectra along the XM lines for 10 and 2 UC. In contrast to the 10 UC film, in which a strongly renormalized band crosses the E_F [Fig. 3(a)] and quasiparticle peaks are well-defined [Fig. 3(b)], the band in the 2 UC film exhibits a diffuse feature despite its much faster dispersion [Fig. 3(c)]. Moreover, the ARPES spectral weight at E_F is strongly suppressed below t_c [Fig. 3(d)], as clearly shown by comparing E_F-symmetrized spectra at the Fermi momenta for various thicknesses [Fig. 3(e)]. Such behavior could be understood by 1D-like fermiology because there is no Fermi-liquid quasiparticle in a 1D system [33,34].

We also compare the ARPES band dispersions with the GGA (black solid lines) and the GGA+DMFT (red open circles) calculations in Figs. 3(a) and 3(c) for the 10 and 2 UC films, respectively. For the 10 UC film, the GGA+DMFT calculations well describes the dispersion, thus Fermi-liquid behavior is expected in this case. On the other hand, for the 2 UC film, the dispersion is surprisingly well fit by the GGA calculations, i.e. the bare band dispersion, which is opposite to our naive expectation that a quantum correlation should play an important role in low-dimensional systems. Note that this behavior is also reminiscent of the single-hole dynamics in cuprate oxides, which differs considerably depending on its

dimensionality [35]. In 2D cuprate $Sr_2CuCl_2O_2$, for example, ARPES spectra show a very narrow band [36]. However, in a 1D cuprate $SrCuO_2$, in which spin and charge degrees of freedom are well separated, the "holon"-branch dispersion is as fast as that of the bare band [35,37].

E. Fermi-surface nesting and possible one-dimensional spin order

Figure 4(a) shows a FS map for the 2 UC LNO film. In our previous study [25], we could observe FS superstructures for compressive and tensile-strained 10 UC LNO films, which were attributed to charge disproportionation and additional SDW fluctuations in three dimension. A FS superstructure can also be observed in the 2 UC film, similar to but much stronger than that in the tensile-strained 10 UC film. In the bulk-like 10 UC film, the superstructure may originate from FS nesting with a $\mathbf{Q} = (1/4,1/4,1/4)$ modulation. However, below t_c, the nesting vector should be modified to $\mathbf{Q} = (1/4,1/4,0)$ or $(1/4,0,0)$ due to the lower dimensionality. According to recent calculations by Lee *et al.* [38], as the LNO film thickness decreases, the spin susceptibility along the (100) direction becomes larger than that along the (110) direction. Thus, we can expect 1D nesting, i.e. $\mathbf{Q} = (1/4,0,0)$. Here, we will neglect the possible checkerboard-type charge ordering present in other bulk nickelates [39,40], because it is not relevant to the 1D electronic structure. In addition, note that since we did not observe any significant signature corresponding to surface reconstruction in the electron diffraction patterns, we may exclude the possibility that surface reconstruction is the origin of the FS superstructure (SM Fig. S1).

If the nesting is strong enough to completely remove the spectral weight at E_F, then the film will have a FS only along one direction. (Note that there will be a twin FS along the perpendicular direction because we can expect that a 90-degree-rotated domain will populate equally.) However, the existence of the FS superstructure implies that the gap does not fully

open. In Fig. 4(b), we depicted schematic diagrams of the FS and its superstructure due to 1D

nesting with $\mathbf{Q} = (1/4,0,0)$. The left diagram demonstrates that there is FS nesting along the k_x

direction, transferring some spectral weight at E_F (represented by thick dashed lines) to the

FS superstructure (represented by thin dashed lines), while the 1D FS along the k_y direction

remains unchanged (represented by solid lines). In the middle diagram, the twin FS and its

superstructure are shown as noted above. As a result, the FS map will be given as in the right

diagram, in good agreement with the experimental FS map shown in Fig. 4(a).

In Fig. 4(c), a possible spin ordering due to the 1D FS nesting is schematically depicted.

The nesting vector $\mathbf{Q} = (1/4,0,0)$ will stabilize a SDW state in which the spins are

antiferromagnetically aligned along the x-axis with an "up-up-down-down" spin pattern,

while it has a ferromagnetic order along the y-axis [38]. If we remove an electron from this

state via an ARPES process, the resulting single hole will have different dynamics depending

on its direction of motion. Hole hopping along the x-axis costs considerable energy to break

the spin-ordering pattern. Thus, the spectral weight around the E_F should be transferred to a

higher binding energy. On the other hand, when the hole hops along the y-axis, its motion is

rather free, making a fast band similar to that from the GGA calculations. As a result, the hole

motion becomes quasi-1D. But, as is well known, Fermi-liquid quasiparticles do not exist in

quasi-1D systems [41-43], thus the spectral weight near the E_F is strongly suppressed and the

bands are quite diffuse. Note that according to the picture in Fig. 4(c), no spin excitation

occurs when the hole moves along the y-axis. Therefore, there should be no well-separated

"spinon" branch, which is consistent with our ARPES spectra shown in Fig. 3(c). Similar

behavior was also observed in a recent ARPES study of a quasi-1D Mo blue bronze, where

spinon and holon branches are smeared into an unexpectedly broad single band [43]. In short,

the single ansatz of 1D FS nesting, which leads to 1D SDW formation, the anomalous

spectral features, i.e. the 1D-like fast band dispersion and the spectral-weight suppression

11

near the E_F below t_c can be described. To confirm this picture, structural studies, such as spin-polarized scanning tunneling microscopy [44] and resonant soft X-ray scattering [22], are immediately suggested.

F. Metal-insulator transition associated with dimensional crossover

Although our ARPES spectra show that a Luttinger-FS persists down to the 1 UC film, numerous studies have reported the insulating properties of such ultrathin LNO films and superlattices [17-24]. To explain the insulating ground state, several mechanisms have been proposed, such as charge disproportionation [20] and Mott transition due to band narrowing by quantum confinement [21]. Our *ex situ* transport measurements also showed an insulating temperature dependence below t_c (SM Fig. S4). However, we can rule out these two possibilities because they should have a full gap. Another possibility is that the insulating behavior originates from the generation of a large percolating cluster of insulating channels in ultrathin films [8]. *In situ* local probe measurements, such as conducting-atomic force microscopy and scanning tunneling microscopy, could be the most effective method to investigate the percolating phenomena. However, such measurements remain challenging with oxide heterostructures. Instead, we observed nearly temperature independent ARPES data of the 3-UC-thick LNO film (SM Fig. S3). If there are significant percolating channels, we might be able to observe a temperature-dependent change in the photoemission spectra due to phase separation [45]. This result suggest, therefore, that percolating channels might be not the origin of the insulating behavior in our ultrathin films.

Disorder effects, such as Anderson localization, play an important role in low-dimensional systems, especially with regard to their transport properties. It is well known that any slight disorder in low dimensions can cause insulating behavior [46,47]. This is consistent with earlier transport studies that emphasize the role of Anderson localization for insulating states

12

[17,18]. However, the localization cannot clearly explain the electronic-structure changes shown in this work; the quasi-1D nature of the electronic structure due to 1D FS nesting remains the dominant factor governing the single-hole dynamics.

IV. CONCLUSION

In conclusion, we directly investigated the change in the electronic structure of ultrathin LNO films by dimensionality control, combining an *in situ* APRES system with state-of-the-art film fabrication. We found anomalous electronic-structure changes in ultrathin films below t_c. The GGA+DMFT calculations show that consideration of the local correlation cannot account for such changes. As a possible origin, we propose the 1D FS nesting to explain the FS superstructure as well as the anomalous electronic structure. Further experimental and theoretical works are necessary to clarify its origin.

[1] S. Ghosh,W. Bao, D. L. Nika, S. Subrina, E. P. Pokatilov, C. N. Lau, and A. A. Balandin, Nat. Mater. **9**, 555 (2010).

[2] Y. Zhang, K. He, C.-Z. Chang, C.-L. Song, L.-L. Wang, X. Chen, J.-F. Jia, Z. Fang, X. Dai,W.-Y. Shan, S.-Q. Shen, Q. Niu, X.-L. Qi, S.-C. Zhang, X.-C. Ma, and Q.-K. Xue, Nat. Phys. **6**, 584 (2010).

[3] J.-P. Locquet, J. Perret, J. Fompeyrine, E. Ma¨chler, J. W. Seo, and G. Van Tendeloo, Nature **394**, 453 (1998).

[4] R. Peng, X. P. Shen, X. Xie, H. C. Xu, S. Y. Tan, M. Xia, T. Zhang, H. Y. Cao, X. G. Gong, J. P. Hu, B. P. Xie, and D. L. Feng, Phys. Rev. Lett. **112**, 107001 (2014).

[5] E. J. Monkman, C. Adamo, J. A. Mundy, D. E. Shai, J. W. Harter, D. Shen, B. Burganov, D. A. Muller, D. G. Schlom, and K. M. Shen, Nat. Mater. **11**, 855 (2012).

[6] K. Yoshimatsu, K. Horiba, H. Kumigashira, T. Yoshida, A. Fujimori, and M. Oshima, Science **333**, 319 (2011).

[7] Y. J. Chang, L. Moreschini, A. Bostwick, G. A. Gaines, Y. S. Kim, A. L. Walter, B. Freelon, A. Tebano, K. Horn, and E. Rotenberg, Phys. Rev. Lett. **111**, 126401 (2013).

[8] Y. J. Chang, C. H. Kim, S.-H. Phark, Y. S. Kim, J. Yu, and T. W. Noh, Phys. Rev. Lett. **103**, 057201 (2009).

[9] M. Imada, A. Fujimori, and Y. Tokura, Rev. Mod. Phys. **70**, 1039 (1998).

[10] J. Chakhalian, A. J. Millis, and J. Rondinelli, Nat. Mater. **11**, 92 (2012).

[11] H. Y. Hwang, Y. Iwasa, M. Kawasaki, B. Keimer, N. Nagaosa, and Y. Tokura, Nature Mater. **11**, 103 (2012).

[12] J. Chaloupka, and G. Khaliullin, Phys. Rev. Lett. **100**, 016404 (2008).

[13] P. Hansmann, X. Yang, A. Toschi, G. Khaliullin, O. K. Andersen, and K. Held, Phys. Rev. Lett. **103**, 016401 (2009).

[14] P. Hansmann, A. Toschi, X. Yang, O. K. Andersen, and K. Held, Phys. Rev. B **82**,

235123 (2010).

[15] M. J. Han, X. Wang, C. A. Marianetti, and A. J. Millis, Phys. Rev. Lett. **107**, 206804 (2011).

[16] N. Parragh, G. Sangiovanni, P. Hansmann, S. Hummel, K. Held, and A. Toschi, Phys. Rev. B **88**, 195116 (2013).

[17] J. Son, P. Moetakef, J. M. LeBeau, D. Ouellette, L. Balents, S. J. Allen, and S. Stemmer, Appl. Phys. Lett. **96**, 062114 (2010).

[18] R. Scherwitzl, S. Gariglio, M. Gabay, P. Zubko, M. Gibert, and J.-M. Triscone, Phys. Rev. Lett. **106**, 246403 (2011).

[19] D. P. Kumah, A. S. Disa, J. H. Ngai, H. Chen, A. Malashevich, J. W. Reiner, S. Ismail-Beigi, F. J. Walker, and C. H. Ahn, Adv. Mater. **26**, 1935 (2014).

[20] A. V. Boris, Y. Matiks, E. Benckiser, A. Frano, P. Popovich, V. Hinkov, P. Wochner, M. Castro-Colin, E. Detemple, V. K. Malik, C. Bernhard, T. Prokscha, A. Suter, Z. Salman, E. Morenzoni, G. Cristiani, H.-U. Habermeier, B. Keimer, Science **332**, 937 (2011).

[21] Jian Liu, S. Okamoto, M. van Veenendaal, M. Kareev, B. Gray, P. Ryan, J. W. Freeland, and J. Chakhalian, Phys. Rev. B **83**, 161102 (2011).

[22] A. Frano, E. Schierle, M. W. Haverkort, Y. Lu, M.Wu, S. Blanco-Canosa, U. Nwankwo, A.V. Boris, P.Wochner, G. Cristiani, H. U. Habermeier, G. Logvenov, V. Hinkov, E. Benckiser, E. Weschke, and B. Keimer, Phys. Rev. Lett. **111**, 106804 (2013).

[23] E. Sakai, M. Tamamitsu, K. Yoshimatsu, S. Okamoto, K. Horiba, M. Oshima, and H. Kumigashira, Phys. Rev. B **87**, 075132 (2013).

[24] P. D. C. King, H. I. Wei, Y. F. Nie, M. Uchida, C. Adamo, S. Zhu, X. He, I. Božovic´, D. G. Schlom, and K. M. Shen, Nat. Nano. **9**, 443 (2014).

[25] H. K. Yoo, S. I. Hyun, L. Moreschini, H.-D. Kim, Y. J. Chang, C. H. Sohn, D. W. Jeong, S. Sinn, Y. S. Kim, A. Bostwick, E. Rotenberg, J. H. Shim, and T. W. Noh, Sci. Rep. **5**, 8746

(2015).

[26] N. Hamada, J. Phys. Chem. Solids **54**, 1157 (1993).

[27] R. Eguchi, A. Chainani, M. Taguchi, M. Matsunami, Y. Ishida, K. Horiba, Y. Senba, H. Ohashi, and S. Shin, Phys. Rev. B **79**, 115122 (2009).

[28] See Supplemental Material at [URL will be inserted by publisher] for clearer presentation of the abrupt electronic-structure changes between 4 and 3 UC by MDC plots.

[29] J. B. Torrance, P. Lacorre, A. I. Nazzal, E. J. Ansaldo, and Ch. Niedermayer, Phys. Rev. B **45**, 8209 (1992).

[30] P. W. Anderson, Science **235**, 1196 (1987).

[31] X. J. Zhou, P. Bogdanov, S. A. Kellar, T. Noda, H. Eisaki, S. Uchida, Z. Hussain, and Z.-X. Shen, Science **286**, 268 (1999).

[32] S. Raj, T. Sato, S. Souma, T. Takahashi, D. D. Sarma, Priya Mahadevan, J. C. Campuzano, M. Greenblatt, and W. H. McCarroll, Phys. Rev. B **77**, 245120 (2008).

[33] T. Giamarchi, *Quantum Physics in One Dimension* (Oxford University Press, 2003).

[34] F. D. M. Haldane, J. Phys. C: Solid State Phys. **14**, 2585 (1981).

[35] C. Kim, A. Y. Matsuura, Z.-X. Shen, N. Motoyama, H. Eisaki, S. Uchida, T. Tohyama, and S. Maekawa, Phys. Rev. Lett. **77**, 4054 (1996).

[36] J. W. Allen, G.-H. Gweon, R. Claessen, and K. Matho, J. Phys. Chem. Solids **56**, 1849 (1995).

[37] B. J. Kim, H. Koh, E. Rotenberg, S.-J. Oh, H. Eisaki, N. Motoyama, S. Uchida, T. Tohyama, S. Maekawa, Z.-X. Shen, and C. Kim, Nat. Phys. **2**, 397 (2006).

[38] S. B. Lee, R. Chen, and L. Balents, Phys. Rev. B **84**, 165119 (2011).

[39] J. A. Alonso, J. L. Garcı´a-Muñoz, M. T. Fernández-Dı´az, M. A. G. Aranda, M. J. Martı´nez-Lope, and M. T. Casais, Phys. Rev. Lett. **82**, 3871 (1999).

[40] M. Medarde, C. Dallera, M. Grioni, B. Delley, F. Vernay, J. Mesot, M. Sikora, J. A.

Alonso, and M. J. Martínez-Lope, Phys. Rev. B **80**, 245105 (2009).

[41] J. D. Denlinger, G.-H. Gweon, J. W. Allen, C. G. Olson, J. Marcus, C. Schlenker, and L.-S. Hsu, Phys. Rev. Lett. **82**, 2540 (1999).

[42] G.-H. Gweon, J. W. Allen, and J. D. Denlinger, Phys. Rev. B **68**, 195117 (2003).

[43] D. Mou, R. M. Konik, A. M. Tsvelik, I. Zaliznyak, and X. Zhou, Phys. Rev. B **89**, 201116(R) (2014).

[44] M. Enayat, Z. Sun, U. R. Singh, R. Aluru, S. Schmaus, A. Yaresko, Y. Liu, C. Lin, V. Tsurkan, A. Loidl, J. Deisenhofer, and P. Wahl, Science **345**, 653 (2014).

[45] F. Chen, M. Xu, Q. Q. Ge, Y. Zhang, Z. R. Ye, L. X. Yang, Juan Jiang, B. P. Xie, R. C. Che, M. Zhang, A. F. Wang, X. H. Chen, D. W. Shen, J. P. Hu, and D. L. Feng, Phys. Rev. X **1**, 021020 (2011).

[46] E. N. Economou, and M. H. Cohen, Phys. Rev. Lett. **25**, 1445 (1970).

[47] P. A. Lee, Rev. Mod. Phys. **57**, 287 (1985).

Fig. 1. (a)-(f) Fermi surfaces (FSs) in the ΓXM (upper panel) and the ZRA (lower panel) planes of tensile-strained LaNiO$_3$ (LNO) films from 10 to 1 unit cells (UC) obtained by angle-resolved photoemission spectroscopy (ARPES). As the thickness changes from 4 to 3 UC, we can see an abrupt fermiology change, i.e. the FSs in the both symmetry planes become nearly identical and consist of two parallel straight lines along the k_x- and the k_y-axes. (g)-(l) ARPES images along the ΓXM (upper panel) and the ZRA (lower panel) lines. To show the changes in band dispersions by thickness control more clearly, the relative intensity maxima in momentum or energy distribution curves (MDCs or EDCs), are plotted with empty circles and triangles, respectively, in (g) and (k). As the thickness is reduced from 4 to 3 UC, the band dispersions change dramatically from those of the 10 UC film. Additionally, they become nearly identical along the ΓXM and the ZRA lines. Thus, a critical thickness t_c between 4 and 3 UC is identified, at which the electronic structures of LNO films under tensile strain qualitatively show a different nature.

Fig. 2. (a) MDC stack plots of the band dispersions for 2 UC along the $X\Gamma X$ (upper panel) and the MXM (lower panel) lines. The blue circles indicate the peak positions in the MDCs. (b) Same as in a but for 10 UC. The dashed lines are guidelines for the comparison of the band dispersions along the $X\Gamma X$ and the MXM lines. In 2 UC, they are almost identical, while quite different in 10 UC. Constant-energy-surface (CES) maps for 2 UC (c) in the ΓXM and (d) in the ZRA planes at a binding energy ranging from 0 to 0.4 eV. All CES maps show pairs of parallel straight lines along the k_x- and the k_y-axes, irrespective of binding energy. These results strongly suggest the quasi-one-dimensional (1D) nature of the electronic structures in LNO films below t_c. CES maps for 1 UC (e) from the generalized gradient approximation (GGA) and (f) from the dynamical mean-field theory combined with the GGA (GGA+DMFT). The e_g-orbital contributions are shown by rainbow image scales in (e). The

CES maps from the GGA calculations show a clear two-dimensional (2D) nature. The fermiology from the GGA+DMFT calculations looks similar to that from the ARPES data; however, slight increase in the binding energy reveals two-dimensional features. The similar cross shapes of CESs at higher binding energies ($\geq$ 0.2 eV) originate from incoherent excitations.

Fig. 3. (a) Band dispersion and (b) EDC stack plot along the *MXM* line for 10 UC. The band structure and a quasiparticle peak at E_F are well-defined. (c),(d) Same as in (a),(b) but for 2 UC. (e) Symmetrized EDC plots with respect to the Fermi level. Below t_c, the band dispersion is much faster but more diffuse than that above t_c. No well-defined quasiparticle peak is observed, and the ARPES spectral weight at the Fermi momentum is strongly suppressed. The black solid lines and the red empty circles represent the dispersion from the GGA and the GGA+DMFT calculations, respectively. For the 10 UC film, the dispersion is well described by the GGA+DMFT calculations with strong electron renormalization. In contrast, for the 2 UC film, it is well fit by the GGA calculations.

Fig. 4. (a) FS map for 3 UC with a nesting vector $\mathbf{Q} \sim (1/4,0,0)$ which shows a corresponding FS superstructure. The map was symmetrized with respect to the mirror planes and plotted using a log scale. Note that a 90-degree-rotated domain would equally populate in the film. (b) Schematic diagrams of a 1D FS and its superstructure. Because the FS is not fully gapped, it is represented by thick dashed lines and its superstructure by thin ones. If we consider equivalent domains, then the final FS and its superstructure will correspond to the rightmost one. (c) Schematic 1D spin-ordering model with $\mathbf{Q} = (1/4,0,0)$ to explain the diffuse but fast 1D band dispersion. In this diagram, a hole produced in an ARPES process is free to hop

along the y-axis, but it costs significant energy to move along the x-axis due to spin-order breaking.
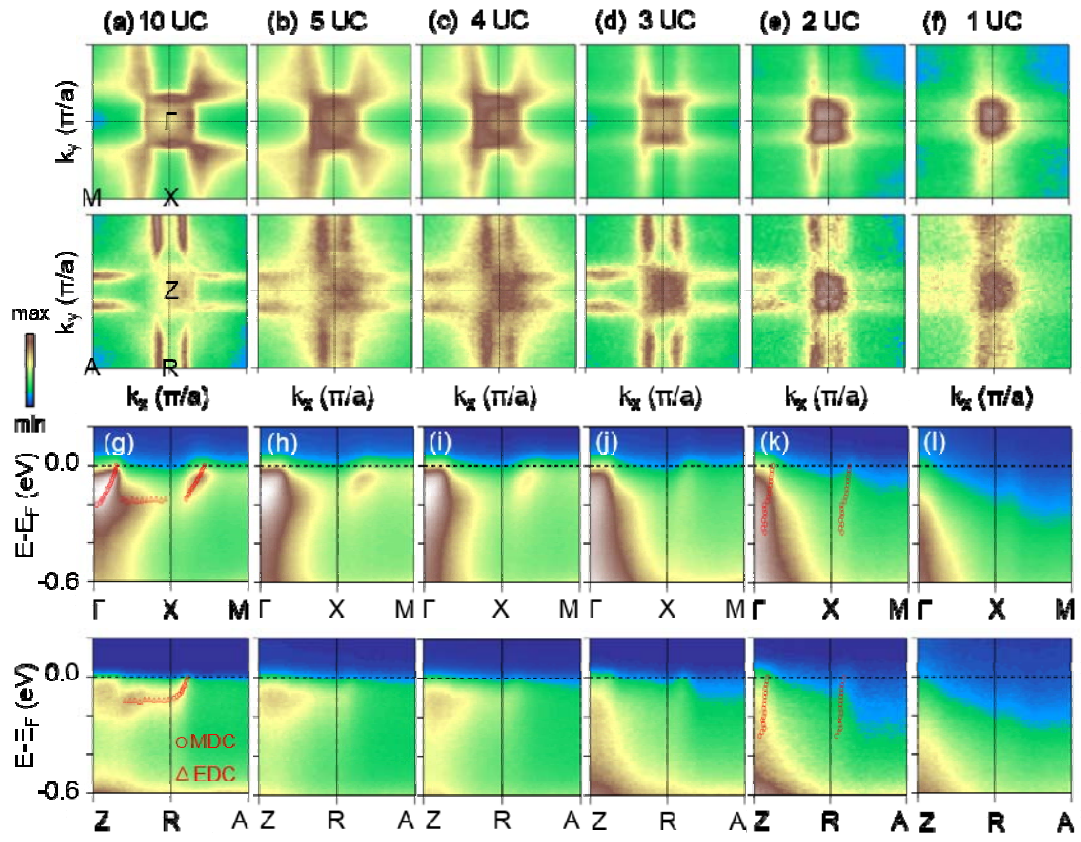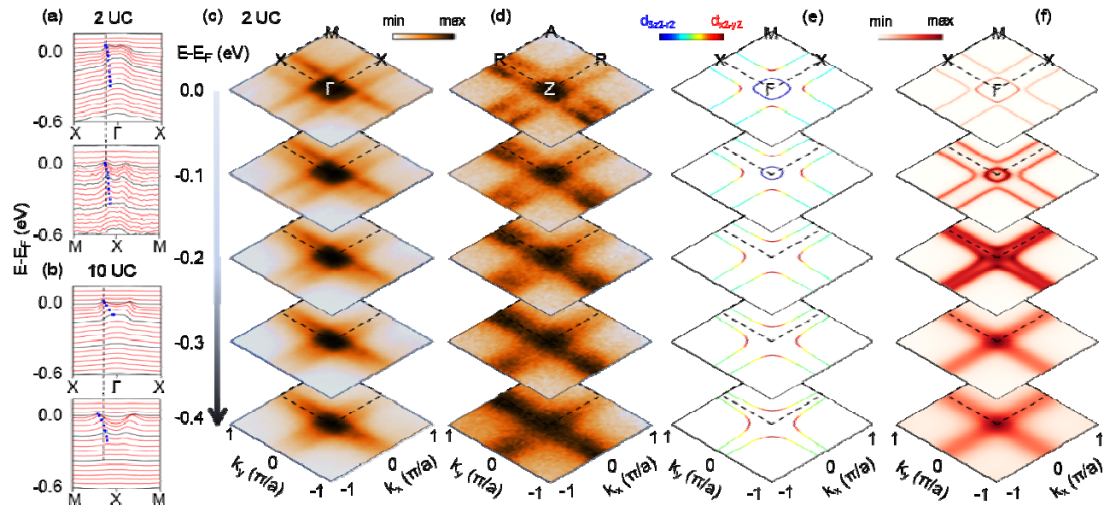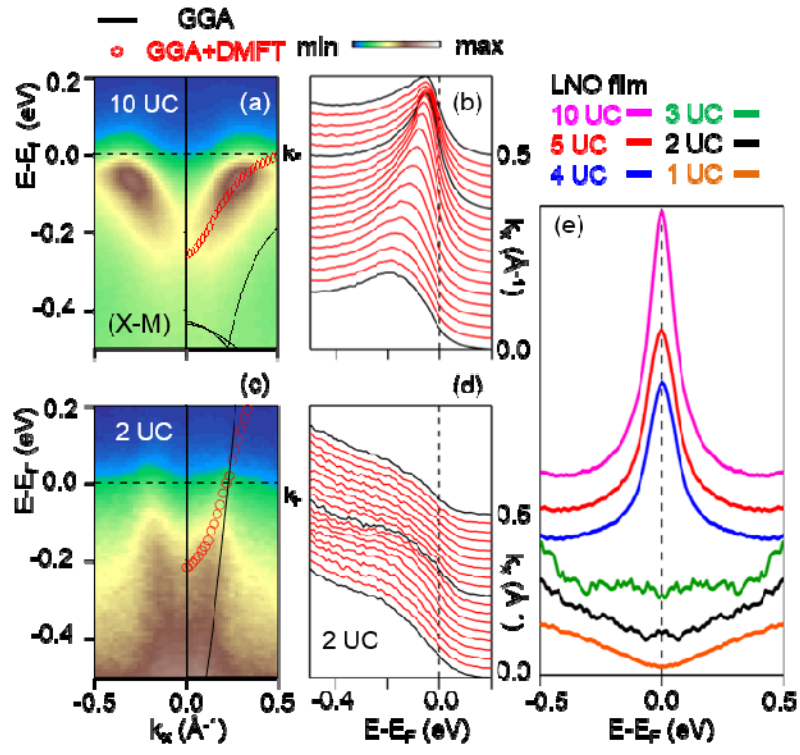
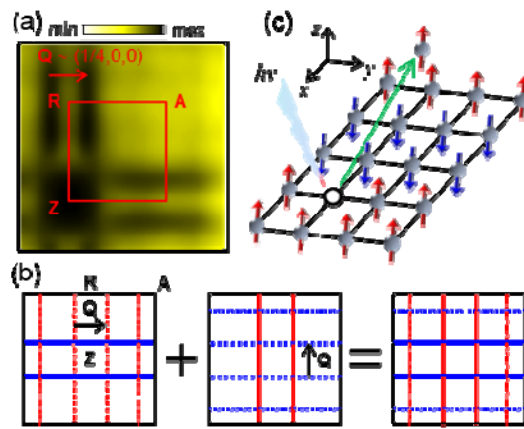Figure 1 H. K. Yoo *et al.*

Figure 2 H. K. Yoo *et al.*

Figure 3 H. K. Yoo *et al.*

Figure 4 H. K. Yoo *et al.*